DNA Nanotechnology

Deutsche Ausgabe: DOI: 10.1002/ange.201511761
Internationale Ausgabe: DOI: 10.1002/anie.201511761

# Bottom-Up Fabrication of Nanopatterned Polymers on DNA Origami by In Situ Atom-Transfer Radical Polymerization

*Yu Tokura[+], Yanyan Jiang[+], Alexander Welle, Martina H. Stenzel, Katarzyna M. Krzemien, Jens Michaelis, Rüdiger Berger, Christopher Barner-Kowollik, Yuzhou Wu,* and Tanja Weil**

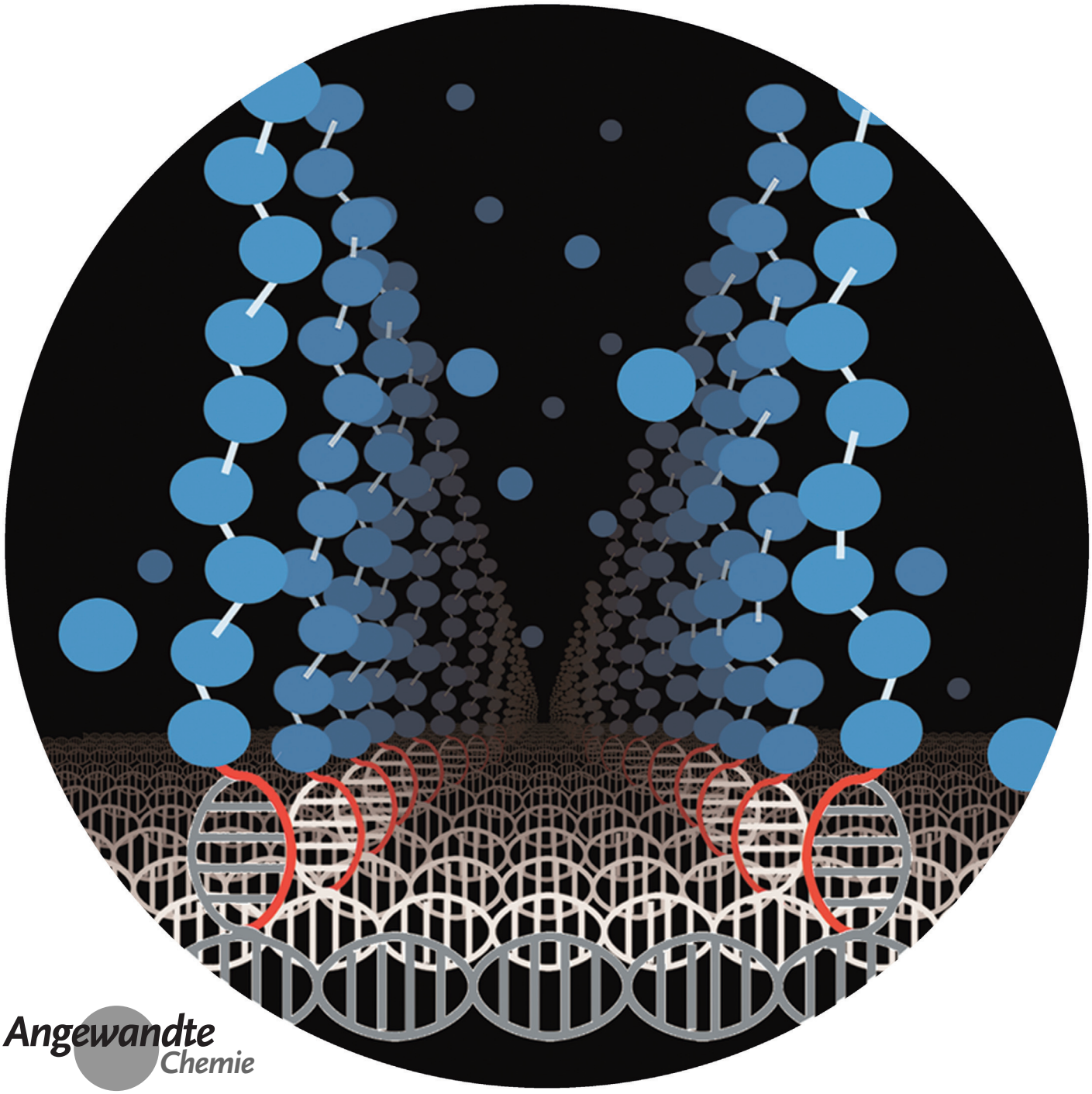


© 2016 Wiley-VCH Verlag GmbH & Co. KGaA, Weinheim

***Abstract:*** *Bottom-up strategies to fabricate patterned polymers at the nanoscale represent an emerging field in the development of advanced nanodevices, such as biosensors, nanofluidics, and nanophotonics. DNA origami techniques provide access to distinct architectures of various sizes and shapes and present manifold opportunities for functionalization at the nanoscale with the highest precision. Herein, we conduct in situ atom-transfer radical polymerization (ATRP) on DNA origami, yielding differently nanopatterned polymers of various heights. After cross-linking, the grafted polymeric nanostructures can even stably exist in solution without the DNA origami template. This straightforward approach allows for the fabrication of patterned polymers with low nanometer resolution, which provides access to unique DNA-based functional hybrid materials.*

Nanofabrication refers to a process that generates patterned structures with a typical resolution of less than 100 nm. The nanopatterning of densely grafted polymers is vitally important to numerous modern technologies, for example, biochips for cell-growth control, micro/nanofluidic systems, and photonic crystal materials.[1] Currently available techniques are mainly based on top-down strategies, such as lithography, which has several limitations, including high instrumental costs and long operation times. Bottom-up strategies in principle enable the fast fabrication of dense polymers. To date, it is still highly challenging to fabricate patterned polymers by bottom-up approaches with low-nanometer resolution. Substantial efforts have been made to induce polymer self-assembly by side-chain supramolecular recognition,[2] although it is impractical to flexibly design the patterns with nanoscale precision. Alternatively, biomacromolecules with regular periodic structures, such as virus capsids, have been derived as reactors allowing for controlled polymerization in their confined nanosized interior cavities.[3] However, the sizes and shapes of polymer structures are seldom tunable by such processes owing to the fixed 3D structures of proteins. On the other hand, DNA is a highly tunable material to create nanostructures. The precise design of artificial DNA sequences and computer-assisted predictions of DNA double-helix folding provide access to a large variety of arbitrary 2D and 3D nanostructures, denoted as DNA origami.[4] This technique has been investigated extensively for the bottom-up nanopatterning of proteins,[5] nanoparticles,[6] and chromophores.[7] Very recently, conductive polymers containing oligonucleotide side chains were successfully assembled on DNA origami by a predefined route.[8] Furthermore, various functional moieties can be incorporated into DNA origami to perform surface-initiated chemical reactions and be characterized by atomic force microscopy (AFM).[9] In this context, capitalizing on DNA origami as a template for the bottom-up fabrication of precise polymer nanopatterns is highly valuable compared to existing systems.

In the current study, we report an in situ polymerization reaction on a DNA origami scaffold for the first time. In situ, or so-called "grafting from" polymerization, offers great opportunities as a method that is often more efficient and leads to denser polymers than the "grafting to" approach, in which polymers are directly conjugated to the surface, resulting sometimes in lower densities because of steric hindrance.[10]

Atom-transfer radical polymerization (ATRP) was selected as a suitable method for polymerization on DNA origami. ATRP is a method of choice to obtain defined polymers with controlled molecular weights, narrow polydispersities, and chain-end functionalities. The reactions proceed in aqueous solution at ambient temperature, which is essential for the stability of the DNA origami structure, and they are applicable to a variety of monomers.[11] To design the nanopatterned ATRP initiators, rectangular DNA origami with dimensions of 70 nm × 100 nm was prepared from the single-stranded M13mp18 DNA and modified staples (see the Supporting Information, Scheme 1 and Figure S1).[4a] Modified staples have additional sequences of 15 nt at the 3′ ends, which are referred to as "sticky sequences" and extend from the surface of the DNA origami. By selecting different modified staples, two different DNA origami patterns were designed: one with two lines (L-origami) and one with four spots (S-origami). To the sticky sequences on these DNA origami patterns, complementary DNA strands with end ATRP-initiator groups (DNA initiator) were hybridized to form the DNA origami macroinitiator (L-origami initiator

[*] Y. Tokura,[+] Y. Jiang,[+] Dr. Y. Wu, Prof. T. Weil
Organic Chemistry III
Macromolecular Chemistry and Biomaterials, Ulm University
Albert-Einstein-Allee 11, 89081 Ulm (Germany)
E-mail: yuzhou.wu@uni-ulm.de
tanja.weil@uni-ulm.de

Y. Jiang,[+] Prof. M. H. Stenzel
Centre for Advanced Macromolecular Design (CAMD)
School of Chemistry, University of New South Wales
Sydney, NSW 2052 (Australia)

Dr. A. Welle, Prof. C. Barner-Kowollik
Preparative Macromolecular Chemistry
Institute for Technical Chemistry and Polymer Chemistry
Karlsruhe Institute of Technology (KIT)
Engesserstrasse 18, 76131 Karlsruhe (Germany)
and
Institute for Biological Interfaces
Karlsruhe Institute of Technology (KIT)
Hermann-von-Helmholtz-Platz 1
76344 Eggenstein-Leopoldshafen (Germany)

Dr. A. Welle
Karlsruhe Nano Micro Facility
Karlsruhe Institute of Technology (KIT)
Hermann-von-Helmholtz-Platz 1
76344 Eggenstein-Leopoldshafen (Germany)

K. M. Krzemien, Prof. J. Michaelis
Institute of Biophysics, Ulm University
Albert-Einstein-Allee 11, 89081 Ulm (Germany)

Dr. R. Berger
Max Planck Institute for Polymer Research
Ackermannweg 10, 55128 Mainz (Germany)

[+] These authors contributed equally to this work.

Supporting information for this article can be found under: http://dx.doi.org/10.1002/anie.201511761.

 © 2016 Wiley-VCH Verlag GmbH & Co. KGaA, Weinheim 

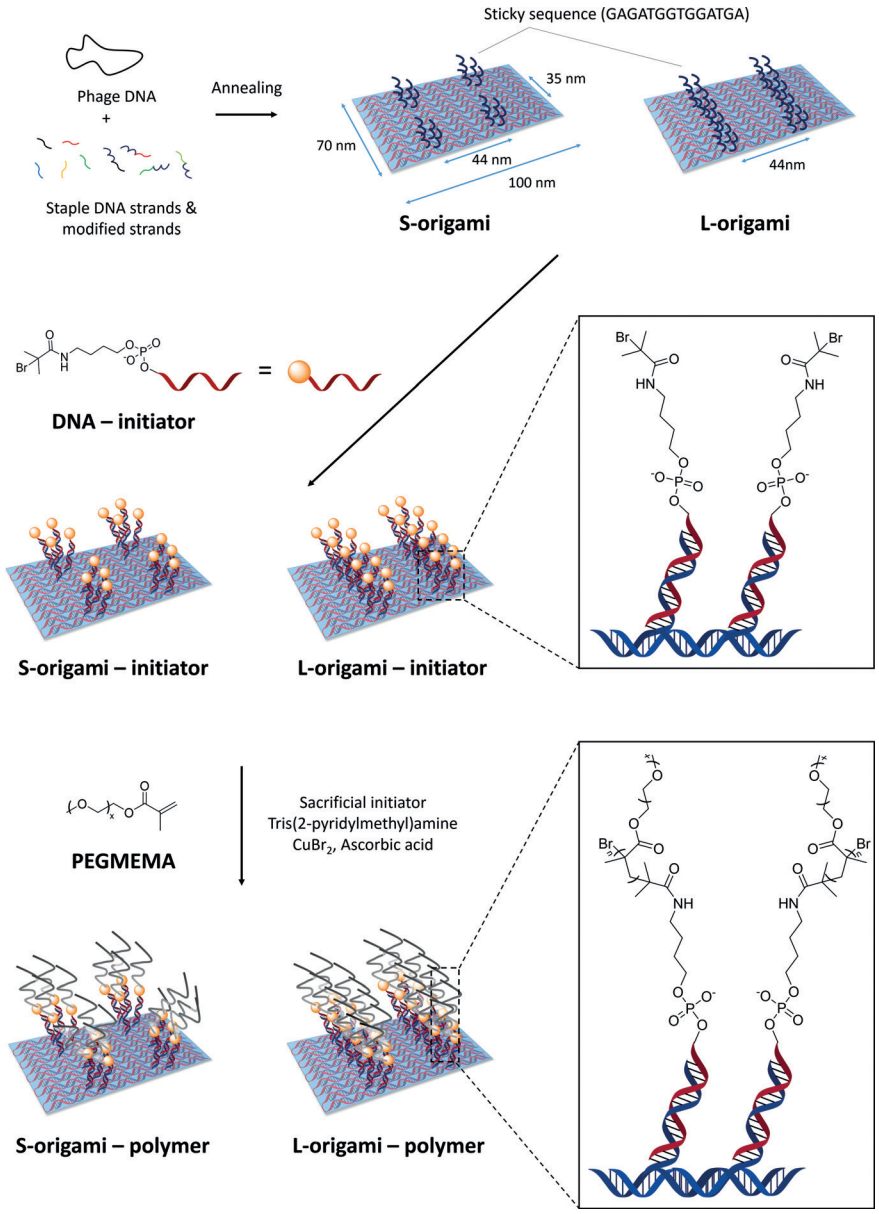


***Scheme 1.*** In situ ATRP on DNA origami.

and S-origami initiator). Although these two patterns were selected as representative examples, even more complicated patterns could be designed following the same approach.

To explore ATRP reactions on DNA origami, the polymerization of poly(ethylene glycol) methyl ether methacrylate (PEGMEMA) was selected owing to its biocompatibility and wide applications in bionanotechnology.[12] Furthermore, the bulky side chain of PEG on the grafted polymer facilitates monitoring the polymer growth on the DNA origami surface by AFM. In solution-based ATRP, the initiator concentration is known to play a pivotal role during the polymerization reaction.[13] Through a systematic examination of the reaction conditions, we found that the reaction only occurred when the initiator concentration was above 10 μM (Figure S2). However, such a high concentration of DNA origami macroinitiators could not be achieved in the reaction mixture owing to the extremely high molecular weight of the DNA origami and the increasing solution viscosity.[14] To overcome this challenge, sacrificial initiators were employed to increase the initiator concentration in the reaction solution, which allowed the generation of a persistent concentration of radicals to establish an ATRP equilibrium. A similar strategy has been reported by Maynard et al.[13] for ATRP reactions with the protein streptavidin as the macroinitiator molecule. Generally, the entire polymerization process was performed in a reaction volume of 20 μL consisting of the DNA origami macroinitiator (50 nM) and the sacrificial DNA initiator (33 μM) in a ratio of 1:665, PEGMEMA (average $M_n$ = 300), $CuBr_2$, and tris(2-pyridylmethyl)amine (TPMA). The reaction mixture was degassed by the freeze–pump–thaw method, which was followed by continuous slow addition of ascorbic acid to generate the reactive catalyst species (Figure S3). After the reaction, the free polymer chains grown from the sacrificial initiators, the catalysts, and unreacted monomers were removed by the PEG-induced precipitation method,[14] and the products (L-origami–polymer and S-origami–polymer) were characterized by agarose gel electrophoresis (AGE) and AFM. AGE analysis showed the different mobility of the DNA origami band (Figure S4). Furthermore, we observed the appearance of new objects at ATRP-initiator-immobilized positions on the DNA origami by AFM (Figure 1). According to the height profile analysis, the average height increase of the DNA origami was 0.55 nm ± 0.02 nm (standard error, S.E.) for L-origami–polymer and 0.56 ± 0.02 nm for S-origami–polymer. Quantitative nanomechanical property mapping (QNM) by AFM revealed that the formed objects have different mechanical properties than the original DNA origami (i.e., a lower Young's modulus and higher adhesion to silicon nitride cantilever), which correspond to the typical surface properties of a polymeric material (softer and more hydrophobic than DNA; Figure 1b). Together these results indicate the successful polymer growth from DNA origami at the desired positions. Remarkably, during the AFM measurement, almost all of the L-origami—polymer deposited on mica showed the polymer-grown surface upside, and hardly any plain surfaces were observed (Figure 1 and Figure S5a). On the other hand, 51 % of the S-origami–polymer molecules


© 2016 Wiley-VCH Verlag GmbH & Co. KGaA, Weinheim

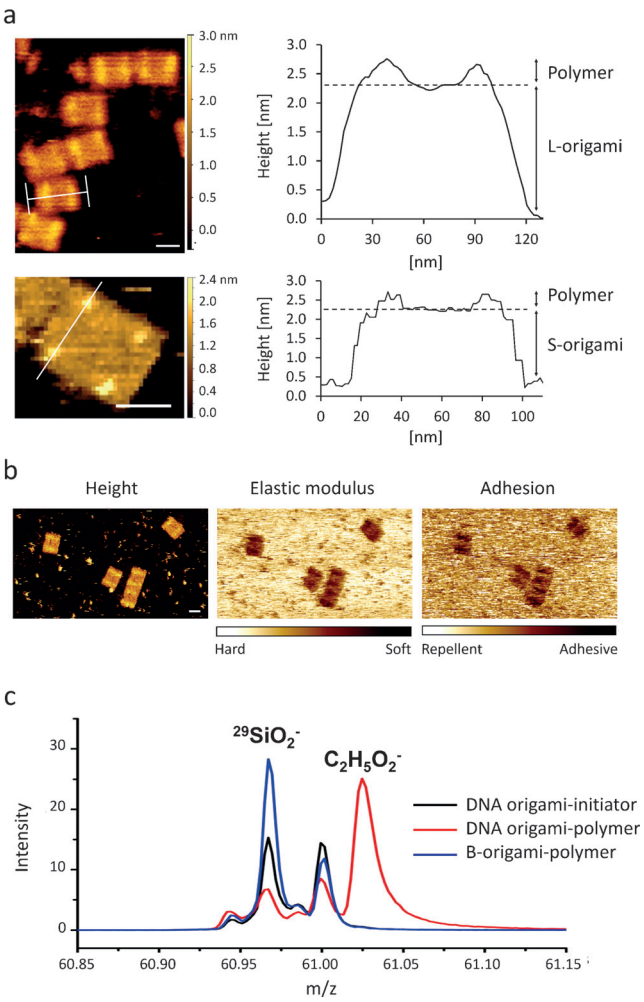


***Figure 1.*** a) AFM images and height profiles of L-origami–polymer (top) and S-origami–polymer (bottom). Scale bars: 50 nm. b) QNM images of L-origami–polymer. c) ToF-SIMS spectrum. $^{29}SiO_2^-$ peaks are due to the mica surface.

were observed to have a polymer surface whereas the others were shown as plain surfaces (Figure S5b). Considering that DNA origami has two surfaces, namely the initiator-immobilized surface and the unmodified plain surface, this result indicates that the grafted polymers had an evident impact on the surface properties of the DNA origami (e.g., in terms of charge, surface topology, and hydrophobicity), thus resulting in a favorable deposition of the negatively charged plain origami side of the L-origami–polymer onto the positively charged mica surface over the polymer-grown side (Figure S5c). In the case of S-origami, the polymer coverage area is three times smaller than for L-origami, and therefore, the surface properties of S-origami were not altered as significantly as those of L-origami, thus no significant orientation preference was observed. This observation is consistent with previous reports by other groups that 2D DNA origami with significant surface decoration will have preferential orientations of deposition.[5]

To further confirm the successful polymerization on DNA origami by a spectrometric method, time-of-flight secondary ion mass spectrometry (ToF-SIMS) analysis was performed. As shown in Figure 1c, the secondary ion derived from the end group of the PEG chain ($C_2H_5O_2^-$) was detected in the purified DNA origami–polymer sample deposited on mica, but not in the sample obtained before the reaction (red and black line in Figure 1c). As the control, DNA origami without modified staples (B-origami) was prepared, mixed with the DNA initiator, and exposed to the same polymerization and purification process (B-origami–polymer, blue line, see Figure S6, Figure S7, and Table S1), from which only significant $PO_3$ and $PO_4$ fragments from DNA species were detected, and no PEG chain peaks were observed. This result clearly indicates that the polymers did not adhere to DNA origami by non-specific interactions.

A major advantage of the bottom-up strategy is the straightforward control of the polymer length without decreasing the conjugation efficiency.[10d] We demonstrated that by changing the molar monomer/initiator ratios (the total amount of initiator in the reaction system), the degree of polymer growth could be tuned. As shown in Figure 2, by

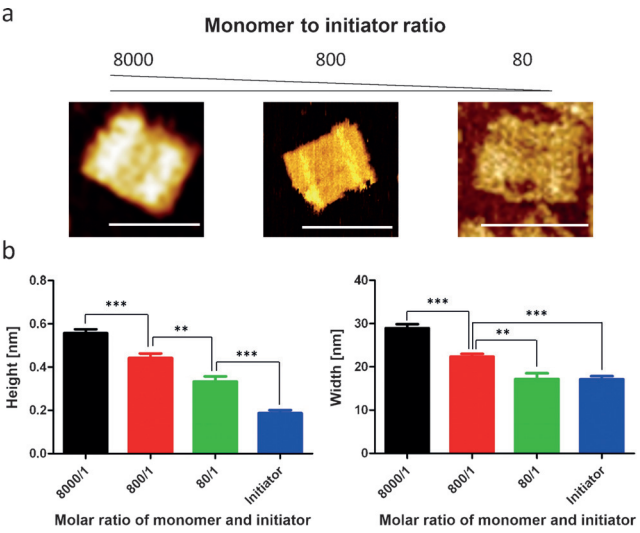


***Figure 2.*** a) AFM images of the polymers on the origami structure made with different monomer/initiator ratios. Scale bars: 100 nm. The average height (b) and width (c) of the grafted polymers on L-origami decrease with a decreasing monomer/initiator ratio. Data represent means ± S.E., $n = 17$. **: $p < 0.001$; ***: $p < 0.0001$.

using monomer/initiator ratios of 8000:1, 800:1, and 80:1, polymers with significantly different heights and widths were obtained. A ratio of 80:1 only gave very thin polymers with an increased height profile (0.33 nm ± 0.02 nm). Increasing the monomer concentration to ratios of 800:1 and 8000:1 resulted in an increase in the heights of the polymer layers by 0.44 nm ± 0.02 nm and 0.55 nm ± 0.02 nm, respectively. However, these heights are still significantly shorter than the distances between adjacent initiator positions (5.8 nm), indicating that the polymers should adopt a mushroom-like collapsed structure.[15]

Finally, to demonstrate the unique prospects of the grafting from polymerization approach, we investigated whether the architecture of the grafted polymeric nano-

 © 2016 Wiley-VCH Verlag GmbH & Co. KGaA, Weinheim 

structures templated by DNA origami could be preserved in the absence of the origami scaffold. This time, PEGMEMA was polymerized on L-origami by the established method in the presence of a cross-linker molecule, PEG dimethacrylate (PEGDMA, average $M_n = 750$; Figure 3a). The cross-linked

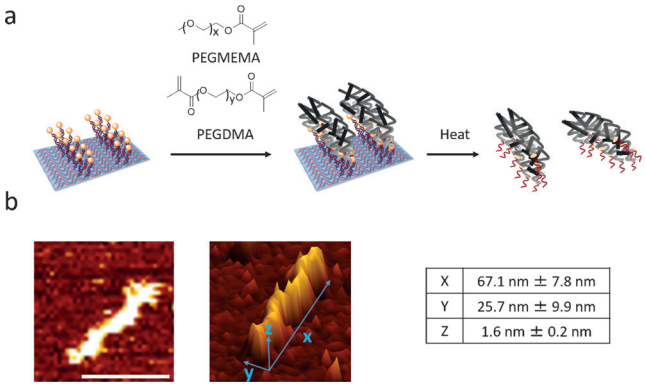


***Figure 3.*** a) Extraction of the cross-linked polymer nanostructure. b) Corresponding AFM image of the cross-linked polymer after decomposition of the DNA origami scaffold (left), 3D view (middle), and the parameters in each direction (right). Scale bar: 50 nm.

polymers had the same shapes and properties on the DNA origami as the polymers that were obtained in the absence of the cross-linker (Figure S8). To remove the DNA origami template, the sample was diluted by a factor of 50 by the addition of water and incubated overnight at 60 °C. The stability of DNA origami is significantly affected by the temperature as well as the $Mg^{2+}$ concentration in the buffer solution. According to AFM, only the cross-linked polymeric structure remained, and no DNA origami structures were observed (Figure 3b and Figure S9). Therefore, this treatment was sufficient to decompose the DNA origami scaffold. The average lengths and widths of the cross-linked polymers were about 67.1 nm ± 7.8 nm and 25.7 nm ± 9.9 nm, respectively. Considering statistical errors, these dimensions are identical to the lengths and widths of the polymers present before removal of the DNA template (length: 68.6 nm ± 1.1 nm; width: 25.3 nm ± 1.0 nm; Figure S8).

In conclusion, the bottom-up fabrication of polymers with precisely designed nanopatterns on a DNA origami template scaffold by in situ ATRP has been reported for the first time. The success of the polymerization was confirmed by AGE, AFM, QNM, and ToF-SIMS. With different surface coverages of the grafted polymers, the surface properties of the DNA origami were altered as demonstrated by their different affinities to mica surfaces and nanomechanical properties. Furthermore, the degree of polymerization could be tuned by varying the monomer/initiator ratio. The approach reported herein paves the way to the bottom-up fabrication of a large variety of nanoscale-patterned polymers with high density and flexibility. Polymerization from DNA origami scaffolds offers various opportunities, such as the application of cross-linkers to fix the polymeric nanostructures to remain intact even after removal of the DNA origami scaffold. In this way, a multitude of nanopatterned polymeric structures of high precision could be grown from DNA origami and stabilized by cross-linking. As the DNA origami technique provides access to almost any arbitrary nanostructure in 2D and 3D, it could in principle be applied for the fast and flexible bottom-up manufacturing of polymers with any nanopattern, such as 2D square- and cross-shaped polymers and even 3D box- and tube-shaped polymers. Therefore, it could be attractive for a broad range of applications, including the fabrication of novel biochips and nanofluidic systems. Furthermore, modifying the different physical, chemical, and mechanical properties of polymers on DNA origami structures opens new avenues to tune the properties of DNA origami, such as increasing the stability of DNA, for example, for cellular studies or introducing additional stimulus responsiveness for developing responsive DNA materials.[10a–c,16] Therefore, we believe that the approach reported herein will further accelerate the application of DNA origami in materials science and biomedicine.[17]

## Acknowledgements

T.W. is grateful to support by the ERC (Synergy Grant 319130-BioQ). C.B.-K. acknowledges continued funding from the Karlsruhe Institute of Technology (KIT) in the context of the Helmholtz BioInterfaces in Technology and Medicine (BIFTM) program. We thank Ulrich Ziener for critical reading of the manuscript and valuable comments.

**Keywords:** atom-transfer radical polymerization · DNA nanotechnology · origami nanostructures · polymerization · self-assembly

**How to cite:** *Angew. Chem. Int. Ed.* **2016**, *55*, 5692–5697
*Angew. Chem.* **2016**, *128*, 5786–5791

[1] a) M. Geissler, Y. N. Xia, *Adv. Mater.* **2004**, *16*, 1249–1269; b) P. T. Hammond, *Adv. Mater.* **2004**, *16*, 1271–1293; c) P. Kim, S. E. Lee, H. S. Jung, H. Y. Lee, T. Kawai, K. Y. Suh, *Lab Chip* **2006**, *6*, 54–59.

[2] M. El Garah, N. Marets, M. Mauro, A. Aliprandi, S. Bonacchi, L. De Cola, A. Ciesielski, V. Bulach, M. W. Hosseini, P. Samorì, *J. Am. Chem. Soc.* **2015**, *137*, 8450–8459.

[3] J. Lucon, S. Qazi, M. Uchida, G. J. Bedwell, B. LaFrance, P. E. Prevelige, T. Douglas, *Nat. Chem.* **2012**, *4*, 781–788.

[4] a) P. W. Rothemund, *Nature* **2006**, *440*, 297–302; b) C. E. Castro, F. Kilchherr, D. N. Kim, E. L. Shiao, T. Wauer, P. Wortmann, M. Bathe, H. Dietz, *Nat. Methods* **2011**, *8*, 221–229; c) V. Linko, H. Dietz, *Curr. Opin. Biotechnol.* **2013**, *24*, 555–561.

[5] a) B. Saccà, R. Meyer, M. Erkelenz, K. Kiko, A. Arndt, H. Schroeder, K. S. Rabe, C. M. Niemeyer, *Angew. Chem. Int. Ed.* **2010**, *49*, 9378–9383; *Angew. Chem.* **2010**, *122*, 9568–9573; b) J. L. Fu, Y. R. Yang, A. Johnson-Buck, M. H. Liu, Y. Liu, N. G. Walter, N. W. Woodbury, H. Yan, *Nat. Nanotechnol.* **2014**, *9*, 531–536.

[6] a) R. Schreiber, J. Do, E. M. Roller, T. Zhang, V. J. Schüller, P. C. Nickels, J. Feldmann, T. Liedl, *Nat. Nanotechnol.* **2014**, *9*, 74–78; b) T. Zhang, A. Neumann, J. Lindlau, Y. Wu, G. Pramanik, B. Naydenov, F. Jelezko, F. Schüder, S. Huber, M. Huber, F. Stehr, A. Högele, T. Weil, T. Liedl, *J. Am. Chem. Soc.* **2015**, *137*, 9776–9779.

 © 2016 Wiley-VCH Verlag GmbH & Co. KGaA, Weinheim 

[7] a) P. K. Dutta, R. Varghese, J. Nangreave, S. Lin, H. Yan, Y. Liu, *J. Am. Chem. Soc.* **2011**, *133*, 11985 – 11993; b) C. X. Lin, R. Jungmann, A. M. Leifer, C. Li, D. Levner, G. M. Church, W. M. Shih, P. Yin, *Nat. Chem.* **2012**, *4*, 832 – 839.

[8] a) J. B. Knudsen, L. Liu, A. L. B. Kodal, M. Madsen, Q. Li, J. Song, J. B. Woehrstein, S. F. J. Wickham, M. T. Strauss, F. Schueder, J. Vinther, A. Krissanaprasit, D. Gudnason, A. A. A. Smith, R. Ogaki, A. N. Zelikin, F. Besenbacher, V. Birkedal, P. Yin, W. M. Shih, R. Jungmann, M. D. Dong, K. V. Gothelf, *Nat. Nanotechnol.* **2015**, *10*, 892 – 898; b) A. Krissanaprasit, M. Madsen, J. B. Knudsen, D. Gudnason, W. Surareungchai, V. Birkedal, K. V. Gothelf, *ACS. Nano* **2016**, *10*, 2243 – 2250.

[9] a) N. V. Voigt, T. Torring, A. Rotaru, M. F. Jacobsen, J. B. Ravnsbaek, R. Subramani, W. Mamdouh, J. Kjems, A. Mokhir, F. Besenbacher, K. V. Gothelf, *Nat. Nanotechnol.* **2010**, *5*, 200 – 203; b) M. Endo, Y. Yang, H. Sugiyama, *Biomater. Sci.* **2013**, *1*, 347 – 360; c) A. H. Okholm, H. Aslan, F. Besenbacher, M. Dong, J. Kjems, *Nanoscale* **2015**, *7*, 10970 – 10973.

[10] a) K. L. Heredia, D. Bontempo, T. Ly, J. T. Byers, S. Halstenberg, H. D. Maynard, *J. Am. Chem. Soc.* **2005**, *127*, 16955 – 16960; b) J. Liu, V. Bulmus, D. L. Herlambang, C. Barner-Kowollik, M. H. Stenzel, T. P. Davis, *Angew. Chem. Int. Ed.* **2007**, *46*, 3099 – 3103; *Angew. Chem.* **2007**, *119*, 3159 – 3163; c) P. De, M. Li, S. R. Gondi, B. S. Sumerlin, *J. Am. Chem. Soc.* **2008**, *130*, 11288; d) Y. Z. Qi, A. Chilkoti, *Polym. Chem.* **2014**, *5*, 266 – 276.

[11] a) K. Matyjaszewski, N. V. Tsarevsky, *Nat. Chem.* **2009**, *1*, 276 – 288; b) D. J. Siegwart, J. K. Oh, K. Matyjaszewski, *Prog. Polym. Sci.* **2012**, *37*, 18 – 37.

[12] S. M. Ryan, G. Mantovani, X. X. Wang, D. M. Haddleton, D. J. Brayden, *Expert Opin. Drug Delivery* **2008**, *5*, 371 – 383.

[13] D. Bontempo, H. D. Maynard, *J. Am. Chem. Soc.* **2005**, *127*, 6508 – 6509.

[14] E. Stahl, T. G. Martin, F. Praetorius, H. Dietz, *Angew. Chem. Int. Ed.* **2014**, *53*, 12735 – 12740; *Angew. Chem.* **2014**, *126*, 12949 – 12954.

[15] N. Backmann, N. Kappeler, T. Braun, F. Huber, H.-P. Lang, C. Gerber, R. Y. H. Lim, *Beilstein J. Nanotechnol.* **2010**, *1*, 3 – 13.

[16] L. Peng, C. Wu, M. You, D. Han, Y. Chen, T. Fu, M. Ye, W. Tan, *Chem. Sci.* **2013**, *4*, 1928 – 1938.

[17] Y. Z. Wu, D. Y. W. Ng, S. L. Kuan, T. Weil, *Biomater. Sci.* **2015**, *3*, 214 – 230.

Received: December 19, 2015
Revised: February 5, 2016
Published online: April 5, 2016

 © 2016 Wiley-VCH Verlag GmbH & Co. KGaA, Weinheim 